

ARTICLE OPEN



Culexarchaeia, a novel archaeal class of anaerobic generalists inhabiting geothermal environments

Anthony J. Kohtz¹, Zackary J. Jay¹, Mackenzie M. Lynes¹, Viola Krukenberg¹ and Roland Hatzenpichler^{1,2}✉

© The Author(s) 2022

Geothermal environments, including terrestrial hot springs and deep-sea hydrothermal sediments, often contain many poorly understood lineages of archaea. Here, we recovered ten metagenome-assembled genomes (MAGs) from geothermal sediments and propose that they constitute a new archaeal class within the TACK superphylum, “*Candidatus* Culexarchaeia”, named after the Culex Basin in Yellowstone National Park. Culexarchaeia harbor distinct sets of proteins involved in key cellular processes that are either phylogenetically divergent or are absent from other closely related TACK lineages, with a particular divergence in cell division and cytoskeletal proteins. Metabolic reconstruction revealed that Culexarchaeia have the capacity to metabolize a wide variety of organic and inorganic substrates. Notably, Culexarchaeia encode a unique modular, membrane associated, and energy conserving [NiFe]-hydrogenase complex that potentially interacts with heterodisulfide reductase (Hdr) subunits. Comparison of this [NiFe]-hydrogenase complex with similar complexes from other archaea suggests that interactions between membrane associated [NiFe]-hydrogenases and Hdr may be more widespread than previously appreciated in both methanogenic and non-methanogenic lifestyles. The analysis of Culexarchaeia further expands our understanding of the phylogenetic and functional diversity of lineages within the TACK superphylum and the ecology, physiology, and evolution of these organisms in extreme environments.

ISME Communications; <https://doi.org/10.1038/s43705-022-00175-8>

INTRODUCTION

In the past two decades, massive efforts in recovering metagenome assembled genomes (MAGs) from environmental samples have resulted in the description of many novel high-ranking archaeal lineages [1, 2]. The current picture of archaeal diversity comprises four superphyla—the Asgard, DPANN, *Euryarchaeota*, and TACK archaea—and it is likely that high-ranking lineages (phylum, class, order) are yet to be discovered [1, 2]. Many archaeal phyla, including *Nanoarchaeota* [3], *Ca. Korarchaeota* [4], *Ca. Geoarchaeota* [5], *Ca. Odinarchaeota* [6], *Ca. Marsarchaeota* [7], *Ca. Nezaarchaeota* [8], and *Ca. Brockarchaeota* [9], were originally discovered in extreme geothermal habitats. While most of these lineages have no cultured representatives, they are often proposed to play important roles in biogeochemical cycles [2, 10].

In lieu of cultures, many lineages are currently best understood via MAGs, which allow for determining their taxonomic placement, inferring their metabolic potential, and generating hypotheses on their ecophysiology that may lead to subsequent in situ studies or eventual cultivation [1, 11]. For example, metagenomics revealed that several lineages within the TACK superphylum encode methyl-coenzyme M reductase (MCR), a hallmark enzyme long-thought to be exclusive to alkane-cycling *Euryarchaeota*. This suggests that the potential for methanogenesis and alkane oxidation are more widespread within the archaeal domain than previously realized [8, 12–15]. Additionally, the potential for anaerobic methylotrophy, a process that in archaea had been solely described in methylotrophic methanogens, was recently

detected in MAGs of non-methanogenic *Ca. Brockarchaeota* [9]. Considering the large diversity of uncultivated taxa revealed by environmental metagenomics, characterizing new archaeal lineages through MAGs is crucial to understanding the phylogenetic and metabolic diversity that exists among archaea and revealing their potential impacts on biogeochemical cycling and ecosystem functioning [16].

Here, using ten MAGs from terrestrial hot spring and deep-sea hydrothermal seep sediments, we report on a new archaeal class, “*Candidatus* Culexarchaeia”. We describe their biogeographic distribution across geothermal systems, evaluate their phylogenetic affiliation through marker gene and functional gene analysis, and describe genes encoding unique protein complexes and versatile metabolic pathways.

MATERIALS AND METHODS

Sample collection, DNA extraction, and metagenome sequencing

Two hot springs located in the Lower Culex Basin (LCB) thermal complex of Yellowstone National Park (YNP) were sampled for molecular and geochemical analyses. At the time of sampling in October 2017, YNP site LCB-003 (44.57763, –110.78957) had a temperature of 72.5 °C and a pH of 6.47, while YNP site LCB-024 (44.57347, –110.79504) had a temperature of 69.4 °C and a pH of 7.79. Surface sediments (~1 cm deep) were collected, immediately frozen on dry ice before transfer to the lab, and subsequently stored at –80 °C until further processing. DNA was extracted from ~1 g of sediment using the FastDNA Spin Kit for Soil (MP Biomedicals) according to

¹Department of Chemistry and Biochemistry, Center for Biofilm Engineering, and Thermal Biology Institute, Montana State University, Bozeman, MT, USA. ²Department of Microbiology and Cell Biology, Montana State University, Bozeman, MT, USA. ✉email: roland.hatzenpichler@montana.edu

Received: 7 April 2022 Revised: 3 September 2022 Accepted: 8 September 2022

Published online: 20 September 2022

manufacturer's instructions (MP Bio). DNA extracts were shotgun sequenced at the Joint Genome Institute (JGI). Truseq libraries were prepared using low input (10 ng for LCB-003) or regular input (100 ng for LCB-024) quantities of DNA. Libraries were sequenced on an Illumina NovaSeq platform using the NovaSeq XP V1 reagent kits, S4 flow cell, following a 2 × 150 indexed run recipe.

Metagenome assembly, binning, and quality assessment

Metagenomic reads for YNP sites LCB-003 and LCB-024 metagenomes were quality filtered according to JGI's analysis pipeline and assembled with SPAdes v3.12.0 [17] with the following settings: -k 33,55,77,99,111 -meta. Assemblies for the Great Boiling Spring (GBS) [18], Washburn Hot Springs (WB) [14], and Guaymas Basin (GB) samples were downloaded from the IMG/M portal [19]. Assembled scaffolds $\geq 2,000$ bp for each metagenome were binned using six different approaches with four different programs, Maxbin v2.2.4 [20], Concoct v1.0.0 [21], Metabat v2.12.1 (with and without coverage) [22], and Autometa v1 (bacterial and archaeal modes, including the machine learning step) [23]. Bins produced from each program were refined with DAS_Tool [24]. In addition, the published MAG JZ-Bin-30, recovered from a metagenome obtained from a geothermal well in the Yunnan province (China) [25, 26], was downloaded from the IMG/M portal. CheckM [27] was used to estimate MAG completeness, redundancy, and relative abundance. tRNAs were identified with tRNAscan-SE [28], using the archaeal-specific covariance models. Optimal growth temperature was predicted for each MAG using Tome, which analyzes proteome-wide 2-mer amino acid compositions [29].

Geochemical analyses

Geochemical data for most sites discussed in this study have been described previously: GBS [18], WB [14], and Jinze Spring (JZ) [25, 26]. The Guaymas Basin (GB) metagenomes were limited in available geochemical data, but the temperature range was 53–83 °C near the time of sampling, based on the temperature profiles measured near the position the sediment core was collected (Supplementary Table 1). For YNP sites LCB-003 and LCB-024 samples for aqueous geochemistry, including dissolved oxygen, dissolved sulfide, dissolved iron, and dissolved gasses (H_2 , CH_4 , and CO_2) were collected as described previously [30] and are available in Supplementary File 7.

Phylogenetic analyses

The 16S rRNA gene sequences encoded in Culexarchaeia MAGs were used in BLASTn searches to screen NCBI and IMG databases for related sequences. Culexarchaeia 16S rRNA sequences were aligned against reference archaeal 16S rRNA sequences and masked using SSU-ALIGN [31], which produced a final alignment of 1376 positions that was used for phylogenetic analyses. Maximum likelihood analysis was performed using IQtree2 [32] v2.0.6 with the nucleic acid model GTR + F + G and 1000 ultrafast bootstraps. A set of 43 single-copy marker proteins (Supplementary File 1) used in a previous phylogenomic study [7], were collected from Culexarchaeia MAGs and archaeal reference genomes. These markers were aligned with MUSCLE [33], trimmed with trimAL [34] using a 50% gap threshold, and concatenated. The final trimmed and concatenated alignment of 10,578 positions was used for phylogenetic analysis. Maximum likelihood analysis was performed using IQ-tree2 [32] v2.0.6 with the LG + C60 + F + G model and 1000 ultrafast bootstraps. Additionally, a set of 46 ribosomal proteins (listed in Supplementary File 1) found in Culexarchaeia MAGs and archaeal reference genomes, was used to construct a second maximum likelihood tree (Supplementary Fig. 1). Sequences were aligned with MUSCLE, trimmed with trimAL using a 50% gap threshold, and concatenated. The final trimmed and concatenated alignment of 7,178 positions was used for maximum likelihood tree reconstruction using IQ-tree2 v2.0.6, the LG + C60 + F + G model, and 1,000 ultrafast bootstraps.

Group 4 [NiFe]-hydrogenases

Catalytic subunits of group 4 [NiFe]-hydrogenases encoded in Culexarchaeia MAGs were subjected to phylogenetic analysis along with a set of reference sequences extracted from the HydDB [35]. Amino acid sequences were aligned using Mafft-LINSi and trimmed using trimAL with a gap threshold of 50%, producing a final alignment of 370 residues. A maximum-likelihood tree was reconstructed using IQ-tree2 v2.0.6 with a best fit model LG + R9 selected according to Bayesian information criterion (BIC), 1,000 ultrafast bootstraps, and option -bnni.

FtsZ-homologs

Reference amino acid sequences from within the tubulin superfamily [36–38] were downloaded from NCBI (accessed May 2021), combined with sequences obtained from the Culexarchaeia MAGs aligned with Mafft-LINSi, and trimmed using trimAL with a gap threshold of 70%. This produced a final alignment of 313 residues. IQ-tree2 v2.0.6 was used for maximum-likelihood analysis with a best-fit model LG + R5 according to BIC and node support was calculated with 1,000 ultrafast bootstraps.

Annotation and reconstruction of metabolic potential

Initial analysis of the metabolic potential of the Culexarchaeia MAGs was performed using the annotations provided by the IMG/M database which uses KEGG, COG, pfam, and enzyme ID databases [19]. Manual refinement of the IMG/M annotations was done by inspection of gene neighborhoods, and identification of conserved domains and motifs through submission of genes to the NCBI conserved domain database [39] and Interproscan (v5.48) [40]. Catalytic subunits of [NiFe]-hydrogenases (COG3261, COG3262, and COG3529) were submitted to the HydDB web portal for classification [35]. Putative transmembrane spanning subunits of novel membrane-bound [NiFe]-hydrogenases (Drh, Ehd, Ehe and Ehg complexes) were predicted with TMHMM [41]. Supplementary File 3 includes a full list of genes used to construct the metabolic model, including the associated KEGG, COG, pfam, Enzyme IDs, and IMG locus tags.

Assessment of key cellular machinery genes and methanogenesis marker proteins

The Culexarchaeia MAGs and reference genomes from Marsarchaeia, Methanomethylia, Geoarchaeia, Nezharchaeia, *Sulfolobales*, *Desulfurococcals*, and *Thermoproteales* were screened for the presence and absence of key cellular machinery proteins, identified in previous work [42–44] using arCOG HMMs [45] and HMMER v3.2 [46]. A set of previously identified methanogenesis marker proteins [15] were also assessed using arCOGs and HMMER (v3.2) as previously described [15]. Following the HMMsearch against Culexarchaeia MAGs and reference archaeal genomes, putative hits (E-value threshold of $1e^{-3}$) for each arCOG were manually inspected through BLASTp searches (default settings) against the NCBI non-redundant database and submitted to the NCBI Conserved Domain Database [39]. Supplementary File 2 provides the data used to construct Fig. 1C and contains the arCOG identifiers used in this analysis along with the presence-absence pattern for each genome.

Supplementary methodology

Cell extraction protocols and FISH experiments are described in the Supplementary Text.

RESULTS AND DISCUSSION

In this manuscript, we largely refer to MAGs using the recently proposed archaeal Genome Taxonomy Database (GTDB, Release 202) nomenclature [47]. However, in the interest of being more accessible in the context of previous work and well-established names in the literature, we also list conventional high-ranking superphylum names (Asgard, DPANN, *Euryarchaeota*, TACK). Parentheses indicate taxa that have undergone significant name changes in the GTDB, but are used interchangeably here (e.g., *Ca. Methanomethylia* (*Ca. Verstraetearchaeota*); *Thermoproteia* (*Cre-narchaeota*)). For simplicity we avoid prefixing candidate taxa with the term “*Ca.*” after they have been introduced.

Recovery of MAGs

Metagenomic analysis of microbial communities from three hot springs sediment samples in Yellowstone National Park (WY, USA), one sediment sample from Great Boiling Spring (NV, USA) [18], and two deep-sea hydrothermal seep sediment samples from Guaymas Basin (Gulf of California) resulted in the recovery of nine MAGs representative of a new archaeal lineage (Table 1). Additionally, a single MAG (JZ-Bin-30), originally recovered from Jinze Hot Spring (Yunnan, China) [25, 26], that was related to these newly retrieved MAGs, was identified in the Integrated Microbial Genomes (IMG) database. Completeness estimates for the ten

Table 1. Summary of Culexarchaeia MAGs used in this study.

Genome ID	Origin	Size (Mbp)	Contigs (#)	Largest Scaffold (bp)	CDS	G + C (%)	Compl. (%) ^a	Redundancy (%) ^a	Coverage	Abund. (%) ^a	tRNAs ^b (#)	OGT ^c (°C)
YNP-LCB-003-016	Yellowstone National Park, WY, USA	2.12	266	105,983	2611	38.7	94.7	0.78	72.1	0.52	37	85
YNP-LCB-024-027	Yellowstone National Park, WY, USA	1.70	42	1,082,165	1779	39.8	97.2	0.93	55.4	0.16	47	83
YNP-WB-040	Yellowstone National Park, WY, USA	1.22	141	137,472	1515	38.9	89.7	0.93	169.6	0.67	31	83
YNP-WB-062	Yellowstone National Park, WY, USA	1.63	189	127,818	2045	39.6	88.7	6.54	102.2	0.41	36	87
JZ-Bin-30	Jinze Hot Spring, Yunnan, China	1.48	33	289,617	1588	32.4	96.7	0.00	16.2	N/A	46	82
GBS-70-058	Great Boiling Spring, NV, USA	1.42	129	206,713	1657	37.0	96.7	0.07	14.7	0.25	45	83
GB-1845-036	Guaymas Basin, Mexico	1.43	130	112,765	1700	37.2	99.0	3.74	17.2	0.35	37	84
GB-1867-005	Guaymas Basin, Mexico	1.98	25	843,365	2245	42.2	99.0	3.74	131.7	1.86	46	91
GB-1867-035	Guaymas Basin, Mexico	2.04	296	32,214	2552	35.0	96.7	7.79	19.5	0.36	41	89
GB-1867-097	Guaymas Basin, Mexico	0.82	175	18,843	1034	38.1	89.7	2.57	13.4	0.23	33	84

YNP Yellowstone National Park, LCB Lower Culex Basin, WB Washburn Hot Springs, WY Wyoming, JZ Jinze Spring, GBS Great Boiling Spring, NV Nevada, GB Guaymas Basin, N/A Not available, CDS Coding sequences, Compl. Completeness, Abund. Abundance, OGT Optimal growth temperature.

^aEstimated with CheckM.

^bDetermined using tRNAscan-SE.

^cPredicted optimal growth temperature determined using Tome.

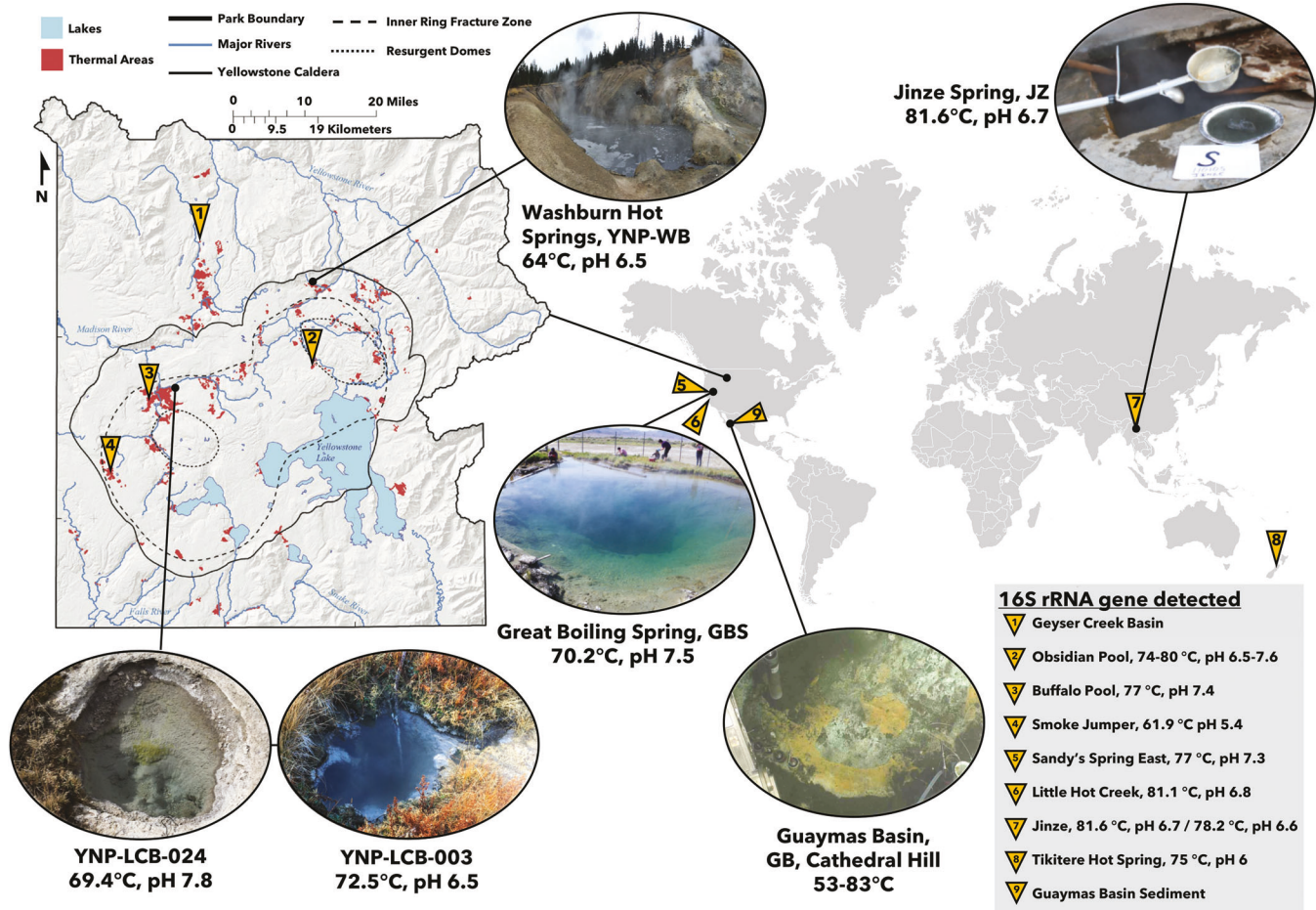


Fig. 2 Biogeography of *Culexarchaeia*. Sites from where *Culexarchaeia* MAGs were recovered and where 16S rRNA gene sequences have been detected. A full list of samples and associated metadata can be found in Supplementary File 8. Yellowstone map modified from ref. [97], GBS picture modified from ref. [18], and JZ picture modified from ref. [25]. Guaymas Basin image courtesy of the Woods Hole Oceanographic Institution.

Biogeography

To explore the biogeographical distribution of *Culexarchaeia*, BLASTn searches were used to screen IMG and NCBI non-redundant databases for related 16S rRNA genes (Supplementary File 8). This revealed that *Culexarchaeia* are globally distributed and are found in circumneutral and slightly acidic pH (5.4–7.8) high temperature (53–83 °C) terrestrial hot spring and deep-sea hydrothermal sediment environments (Fig. 2). A small number of 16S rRNA gene sequences were retrieved from deep-sea hydrothermal seep sediment samples in Guaymas Basin with lower temperatures (15 °C; Supplementary File 8). However, the Guaymas hydrothermal system experiences rapidly fluctuating temperature gradients (up to 100 °C over 50 cm depth) as hydrothermal waters percolate through the sediments [49] (Supplementary Table 2). Consistent with the presence of *Culexarchaeia* in geothermal environments, the predicted optimal growth temperature based on amino acid composition [29] is above 80 °C for all MAGs with an average of 85 °C (Table 1). Furthermore, all MAGs encode the hyperthermophile-specific enzyme reverse gyrase (Supplementary File 2) that is important for growth at high temperatures [50, 51].

We attempted to visualize *Culexarchaeia* cells in cell extracts from sediment slurries of YNP sites 003 and 024 via catalyzed reporter deposition fluorescence in situ hybridization (CARD-FISH) using a newly designed oligonucleotide probe but were unsuccessful. The low relative abundance of *Culexarchaeia* in YNP sites LCB-003 and LCB-024 (0.52% and 0.16% abundance, respectively; Table 1) may have contributed to our inability to detect them. Alternatively, the

failure to detect *Culexarchaeia* cells could be due to suboptimal probe accessibility, an inability to penetrate the archaeal cell wall under the permeabilization conditions tested, or low ribosome content of relatively inactive cells.

Comparison of key cellular machinery proteins encoded by *Culexarchaeia*

To better understand the differences between *Culexarchaeia* and their closest relatives within the TACK superphylum, we surveyed publicly available genomes within the Geoarchaea, Marsarchaea, Methanomethylicia, Nezaarchaea, and *Thermoproteia* (*Crenarchaeota*), for the presence or absence of proteins involved in key cellular processes (Fig. 1C). These marker proteins have been used in previous studies to delineate differences between high-ranking archaeal taxa [42–44] and include archaeal-specific ribosomal proteins, topoisomerases, histones (H3/H4), proteins involved in DNA replication (DNA PolD), DNA repair, cell division, and cytoskeletal proteins. This analysis revealed a lineage-specific presence-absence pattern for *Culexarchaeia* that differentiates them from other TACK lineages (Fig. 1C). In particular, a unique set of cell division and cytoskeletal proteins were found to be encoded in *Culexarchaeia* MAGs.

Culexarchaeia encode a unique array of cell division and cytoskeletal proteins

Many lineages in the TACK superphylum (Bathyarchaea, *Desulfurococcales*, Geoarchaea, Marsarchaea Nezaarchaea, *Nitrosophaeria* (*Thaumarchaeota*), and *Sulfobolales*) encode a full

complement of the ESCRT-III related cell division proteins [52] (CdvABC; Fig. 1C). Methanomethylia, the closest relative to Culexarchaea, has previously been noted to only encode CdvB and CdvC. This is consistent with our expanded analysis of recently discovered Methanomethylia representatives [1, 8, 26]. In contrast, all Culexarchaea MAGs only encoded CdvC homologs, which suggests Culexarchaea may use an alternative mechanism for cell division.

In bacteria, the highly conserved FtsZ tubulin protein mediates the formation of a dynamic division ring during cell division [36]. Many archaea (including most members of the *Euryarchaeota*, DPANN, and Asgard, along with a small number of TACK lineages) also encode homologs of the FtsZ tubulin protein, which is critical for cell division [36]. Divergent FtsZ homologs encoded by *Haloferax volcanii*, later termed CetZ, were found to not be directly involved with cell division, but instead have roles in maintaining cell shape and motility, which highlights the functional diversity present in this family of proteins [37]. Previously, FtsZ homologs had only been noted in other more distantly related TACK lineages including Bathyarchaea, Caldarchaeles (Aigarchaeota), Korarchaea, and *Nitrososphaeria* (*Thaumarchaeota*) [52, 53]. Most of these TACK lineages each encode at least one homolog that clusters with canonical FtsZ1 and/or FtsZ2 from other archaea, which suggests that these proteins likely play a similar role in cell division. Furthermore, Korarchaea, Bathyarchaea, and *Nitrososphaeria* (*Thaumarchaeota*) also encode non-canonical FtsZ-like sequences that have a yet undetermined role in cellular division or cellular shape maintenance [36] (Supplementary Fig. 3).

Members of the Culexarchaea were found to encode a homolog of FtsZ, a protein that is absent in all closely related TACK lineages with the exception of two *Sulfolobales* representatives, which have previously been noted to encode highly divergent and extended proteins belonging to a cluster termed FtsZL1 [38] (Fig. 1C, Supplementary Fig. 3). Compared to other FtsZ clades, the Culexarchaea FtsZ-like sequences form a new, deeply branching clade that is distinct from other known tubulin family homologs and branches between the archaeal FtsZ2 group and CetZ group (Supplementary Fig. 3). Culexarchaea FtsZ-like sequences cluster with other uncharacterized sequences from the Thermoplasmata, Bathyarchaea, Geothermarchaeales, and unclassified Thermoproteia. This novel clade of FtsZ-like proteins represented by Culexarchaea sequences will require experimental characterization to determine its role in cellular division, cellular shape maintenance, or motility.

In contrast to the Cdv and FtsZ mediated cell division strategies, the cell division and cytoskeletal proteins encoded by the *Thermoproteales* have long been a curiosity because, unlike closely related orders within the *Thermoproteia* (*Crenarchaeota*), they do not encode homologs of the CdvABC or FtsZ proteins [54]. Instead, cell division and cellular organization in the *Thermoproteales* have been proposed to rely on homologs of actin (termed crenactin) and several conserved actin-related cytoskeleton proteins (termed arcadins) [54] (Fig. 1C). Based on immunostaining of *Pyrobaculum caldifontis*, arcadin-1, arcadin-3, and arcadin-4 were suggested to play auxiliary roles in cell division and cellular shape maintenance, while arcadin-2 was localized in the center of cells between segregated nucleoids, which suggests that it may play a more direct role in cytokinesis [54]. Culexarchaea MAGs recovered from marine environments contained a similar set of proteins (encoding for crenactin, arcadin-1, arcadin-2, and arcadin-4). In contrast, the terrestrial Culexarchaea MAGs and only encoded arcadin-1, but not crenactin (Supplementary File 2). A few mesophilic members within the Methanomethylia order Methanomethyliales also encode crenactin, while all other Methanomethylia genomes analyzed did not encode crenactin (Supplementary File 2). In addition, no arcadin-related proteins were identified in our arCOG survey of Methanomethylia genomes. A BLASTp search against

the non-redundant database using default settings and the Culexarchaea crenactin sequences as queries revealed that these sequences are more similar to those found in the TACK (e.g., Methanomethylia and Caldarchaeles) than to those in the Asgard archaea, which are more similar to eukaryotic actin sequences [55].

The set of cell division, cell shape, and cytoskeleton proteins encoded by the Culexarchaea suggests that they have a unique cell division and maintenance process. Similarly, members of the Caldarchaeles (Aigarchaeota) have been noted to encode a unique complement of cell division (FtsZ2, CdvBC) and cytoskeletal proteins (Crenactin, arcadin-1, arcadin-2) [56]. Likewise, some Asgard archaea (e.g., Heimdallarchaeota, Odinararchaeota) have been found to encode a mixture of proteins possibly involved in cell division machinery (CdvBC in addition to FtsZ1 and/or FtsZ2) and actin-like sequences that are closely related to eukaryotic homologs [1, 52]. It is yet unknown if, or how, these diverse systems interact with each other during the cell cycle [43, 56]. All together, these data suggest that Culexarchaea, along with other TACK and Asgard lineages, are critical to understanding the diversity and evolution of cell division and cytoskeletal proteins within the *Archaea*.

Metabolic potential of Culexarchaea

Culexarchaea have the potential to live a generalist lifestyle, with the ability to metabolize a variety of substrates including proteins, amino acids, fatty acids, sugars, and methyl compounds (Fig. 3; Supplementary File 3).

Peptide degradation and fermentation

Culexarchaea encode peptide and amino acid transporters that can import exogenous peptides or amino acids that can be catabolized to their respective 2-oxoacids via encoded peptidases and amino-transferases [57, 58]. Ferredoxin oxidoreductases (POR, IOR, KOR) can then convert these 2-oxoacids to their respective Acyl-CoA substrate and reduce a low-potential ferredoxin [58, 59]. Culexarchaea encode multiple Acyl-CoA synthetases that can convert the Acyl-CoA substrates to organic acids and generate ATP via substrate level phosphorylation [58, 59]. Culexarchaea also encode multiple aldehyde-ferredoxin oxidoreductases (AOR) and alcohol dehydrogenases that could act to interconvert organic acids to aldehydes and aldehydes to alcohols, respectively [59–61]. This would remove excess reducing equivalents (NAD(P)H and/or reduced ferredoxin) produced during fermentation. Alternatively, or in addition to, reduced ferredoxins produced by ferredoxin oxidoreductases could also be oxidized by a membrane bound group 4g [NiFe]-hydrogenase concomitantly with H₂ production and the transport of ions outside of the cell (Fig. 3). This scenario would be akin to the metabolism of *Pyrococcus furiosus*, which uses a membrane bound hydrogenase and ATP synthase to conserve energy during hydrogenogenic fermentation [62]. Additional fermentative capacity is possible through the conversion of pyruvate to lactate or alanine through the activity of lactate dehydrogenase (GlcD) or alanine dehydrogenase (Aladh), respectively.

Cyanophycin degradation

All terrestrial MAGs and one marine MAG encode cyanophycinase, a peptidase capable of degrading cyanophycin, a carbon and nitrogen storage polymer [63]. Cyanophycin is commonly found in cyanobacteria and some heterotrophic bacteria and is composed of repeated aspartate and arginine dipeptides [64]. After degrading cyanophycin polymers, Culexarchaea could further metabolize arginine via the arginine deiminase pathway [65] (*arcA*, *arcB*, *arcC*; Fig. 3) to generate ATP, while aspartate could be used in central metabolism via aspartate aminotransferase, converting it to the TCA intermediate oxaloacetate. To the best of our knowledge, cyanophycin degradation by archaea has had

found in geothermal environments, including methylotrophic methanogens, methylotrophic bacteria, or the recently identified Brockarchaeota [9].

Together, these findings suggest that Culexarchaeia are incapable of methanogenesis, and that the WLP would confer metabolic flexibility by acting as a major hub for the entry and exit of multiple substrates. Specifically, if operating in the reductive direction, acetogenesis could occur from CO₂, formate, or methylated compounds (potentially trimethylamine or quaternary amines) (Fig. 3). Formate could be produced through the activity of pyruvate-formate lyase (PflD), formamidase (FmdA), or through interconversion of formaldehyde and formate by aldehyde-ferredoxin oxidoreductases (AOR; Fig. 3). Alternatively, the WLP could be used in the oxidative direction to oxidize Acetyl-CoA or methylated compounds to CO₂ or formate. Culexarchaeia may also use the WLP for protein degradation because they encode serine hydroxymethyltransferase, which can produce a methylene-H₄MPT and glycine. The glycine cleavage system (GCS) could then convert glycine to methylene-H₄MPT, CO₂, and NH₃ [70] (Fig. 3).

Beta-oxidation

Culexarchaeia encode genes for the metabolism of fatty acids through beta-oxidation. This includes medium chain Acyl-CoA dehydrogenases (Acadm), electron transfer flavoproteins (EtfAB), Enoyl-CoA hydratase (Crt), 3-hydroxybutyryl-CoA dehydrogenase (FadB), and Acetyl-CoA C-acetyltransferase (AtoB) [71]. Acetyl-CoA produced by this pathway could then be metabolized by oxidation through the WLP or by Acyl-CoA synthetases to produce ATP through substrate level phosphorylation (Fig. 3). Additionally, electron transfer flavoproteins and Acyl-CoA dehydrogenase may form an electron-bifurcating complex (EtfAB-Acadm), as was previously suggested for fatty acid-degrading *Firmicutes* [72].

Carboxydorotrophy

Culexarchaeia MAGs encode putative aerobic carbon-monoxide dehydrogenases (CoxLMS), which suggests a capacity for carboxydorotrophy through this enzyme complex. Culexarchaeia also encode genes involved in molybdopterin cofactor biosynthesis (Fig. 3), which could be involved with such a molybdoenzyme. However, consistent with an analysis of Cox proteins in Caldarchaeales (Aigarchaeota) and a broader analysis of form I Cox proteins in bacteria and archaea, all Culexarchaeia CoxL homologs lack conserved active site residues (VAYRCSFR) found in other characterized Cox proteins and do not cluster with other characterized form I Cox proteins. Together, this suggests these enzymes may use an alternative substrate [73–75]. However, carboxydorotrophic potential in Culexarchaeia may exist via a [NiFe]-hydrogenase complex that interacts with carbon monoxide dehydrogenase subunit A (CdhA; discussed below).

Gluconeogenesis, RuMP Pathway, TCA cycle, and Nucleotide Salvage Pathway

Culexarchaeia encode important enzymes involved in gluconeogenesis, including phosphoenolpyruvate carboxykinase (PEPCK) and pyruvate:phosphate dikinase (PpdK) for the production of phosphoenolpyruvate (PEP) from oxaloacetate and pyruvate, respectively [76]. While they lack a gene for phosphofructokinase, all MAGs encode fructose bisphosphate aldolase/phosphatase (Fbpa) [77]. Together, this suggests Culexarchaeia are capable of gluconeogenesis [76].

Culexarchaeia have the potential to metabolize a variety of sugars and aldehydes. Several MAGs encode the proteins necessary for using fructose or galactose, which could be converted to fructose-6-phosphate for entry into the ribulose monophosphate (RuMP) pathway (Fig. 3). The RuMP pathway could be used for formaldehyde assimilation/detoxification or biosynthesis of nucleotides [78]. Alternatively, formaldehyde produced by 6-phospho-3-hexuloisomerase (HxIB) could be converted to formate via an aldehyde:ferredoxin

oxidoreductase and then enter the THF branch of the WLP via formate-tetrahydrofolate ligase (Fhs). A single marine MAG, GB-1867-005, encoded a formaldehyde-activating enzyme (Fae) that could incorporate formaldehyde into the H₄MPT branch of the WLP. Glyceraldehyde may be scavenged through conversion to glycerate by an aldehyde-ferredoxin oxidoreductases and glycerate could subsequently be converted to 2-phosphoglycerate by glycerate kinase (Gck) (Fig. 3).

Culexarchaeia encode an incomplete tricarboxylic acid (TCA) cycle that may function as a hub for protein fermentation and conversion of TCA intermediates (malate and oxaloacetate) to pyruvate for gluconeogenesis or conversion to Acetyl-CoA (Fig. 3). Peptide degradation could produce 2-oxoglutarate and glutamate through the activity of aminotransferases and peptidases, respectively. Then, glutamate dehydrogenase (Gdh) could facilitate the interconversion of these substrates. 2-oxoglutarate could be metabolized to produce reduced ferredoxin and succinyl-CoA via 2-oxoglutarate:ferredoxin oxidoreductase (KOR). Succinyl-CoA could then be stepwise converted to succinate, fumarate, and malate through the activities of succinyl-CoA synthetase (SucCD), fumarate reductase (TfrA), and fumarate hydratase (FumAB), respectively (Fig. 3). Malate could be converted to pyruvate by the decarboxylating malic enzyme (MaeA) and enter gluconeogenesis through the conversion to PEP by pyruvate:phosphate dikinase (PpdK). Similar to Methanomethylia, two marine MAGs encode a full nucleotide salvage pathway that includes Ribulose 1,5-bisphosphate carboxylase (RbcL) for conversion of adenosine monophosphate (AMP) to 3-phosphoglycerate (3-PG), which could be metabolized to acetyl-CoA [12].

Extensive capacity for H₂-cycling and many potential electron bifurcating/confurcating complexes

The large number of hydrogenases and putative electron-bifurcating complexes encoded by Culexarchaeia MAGs suggest that these enzymes are important in their metabolism. Flavin-based electron bifurcation involves the coupling of an exergonic redox reaction to drive an endergonic redox reaction [79]. Electron bifurcation has been found to be important in balancing redox carriers within the cell and increasing efficiency of cell metabolism, particularly for anaerobic organisms that grow on low energy-yielding substrates [80, 81]. Culexarchaeia encode five different potential electron bifurcating complexes, which places them among a small number of genomes found to encode more than three bifurcating complexes. These enzymes may provide advantages in energy efficiency and competition over low energy-yielding substrates in situ [79–81].

Culexarchaeia encode multiple group 3 and 4 [NiFe]-hydrogenases, which indicates that they could either produce or consume H₂. The group 3c [NiFe]-hydrogenase (MvhADG) may form a bifurcating complex with HdrABC, as found in other diverse archaea, which allows for the oxidation of H₂ to be coupled to the reduction of ferredoxin and a disulfide compound [82]. Alternatively, given the lack of FrhAG in Culexarchaeia MAGs, HdrABC could form a confurcating complex with FrhB, thus coupling the oxidation of a disulfide and ferredoxin to the reduction of F₄₂₀, similar to a scenario proposed for *Methanoperedens* that don't encode FrhAG [83]. Culexarchaeia also encode three other complexes with the potential to perform electron bifurcation: HdrA2B2C2 (discussed below), EtfAB-Acadm (discussed above with beta oxidation), and NADH-dependent ferredoxin:NADP⁺ oxidoreductase (NfnSL; Fig. 3). By coupling the oxidation of NAD(P)H with the reduction of NAD(P)⁺, this enzyme could play a key role in cellular redox balancing [84].

Culexarchaeia encode a group 3b [NiFe]-hydrogenase that may couple the reversible oxidation of NADPH to the reduction of protons to evolve H₂ [85]. Characterization of the group 3b [NiFe]-hydrogenase in *Pyrococcus furiosus* revealed that it had sulfhydrylase activity. This would allow the cell to couple the oxidation of NADPH with the reduction of elemental sulfur (S⁰) or

polysulfide to H₂S [85, 86]. Thus, Culexarchaeia may be involved in sulfur cycling through the activity of this potential sulfhydrogenase. Reduced ferredoxin produced through fermentative metabolism could be oxidized by a membrane-bound group 4g [NiFe]-hydrogenase, coupled to the translocation of ions and the production of H₂ (Fig. 3). Culexarchaeia also encode a novel group 4 [NiFe]-hydrogenase (termed Ehe, discussed below) that may interact with disulfides, CO, or succinate. Furthermore, the production of H₂ (or formate) by Culexarchaeia could potentially form the basis of syntrophic interactions with other community members through the exchange of these compounds.

An expanded diversity of potential HdrB-interacting hydrogenases

A recent evaluation of MAGs affiliated with the Methanomethylica, the closest relatives to Culexarchaeia, revealed genes encoding a novel membrane bound [NiFe]-hydrogenase complex (termed Ehd) that were co-located with genes encoding heterodisulfide reductase subunits (HdrBC) and an ion antiporter subunit [15] (Fig. 4B, F). This Ehd complex was suggested as an alternative pathway to couple the oxidation of H₂ to the reduction of the heterodisulfide CoM-S-S-CoB and translocation of ions outside the cell, which would allow for energy conservation during methylotrophic methanogenesis [15]. A similar membrane-bound hydrogenase complex (termed Ehe here) is encoded in Culexarchaeia MAGs (Fig. 4A, E). The Ehd and Ehe gene clusters have the same core structure containing genes for a [NiFe]-hydrogenase complex, HdrBC, and an ion antiporter subunit. However, the genes encoding the Ehe complex are co-located with genes encoding succinate dehydrogenase subunit A (SdhA), carbon monoxide dehydrogenase subunit A (CdhA), a predicted bifurcating heterodisulfide reductase complex (HdrA2B2C2) [87], and a glycine cleavage protein H (GcvH). This suggests that carbon monoxide or succinate oxidation could be coupled to the reduction of protons and the translocation of ions to the outside of the cell. Thermodynamics of succinate oxidation coupled to H₂ production indicate that this reaction becomes favorable at temperatures >65 °C [88], which aligns with some of the high-temperature environments that Culexarchaeia inhabit (50–83 °C). Additionally, CO is a common trace gas in geothermal systems and could potentially be oxidized by this complex and coupled to the reduction of protons to H₂ to fuel carboxydrotrophic growth [89].

Alternatively, H₂ oxidation could also be coupled to the reduction of an unknown disulfide (via HdrB) that could be generated through the activity of the HdrA2B2C2 or HdrABC-MvhADG bifurcating complexes. The identity of this disulfide is unknown, but Culexarchaeia lack a full biosynthetic pathway for CoM and CoB, which suggests that an alternative disulfide may be used. The GcvH protein, encoded within the Ehe gene cluster, typically functions in the glycine cleavage pathway to coordinate a disulfide containing lipoyl moiety [90, 91]. This suggests GcvH could play a similar role in coordinating a disulfide containing moiety during potential interactions with HdrB and/or the HdrA2B2C2 bifurcating complex. Determining directionality of the reaction catalyzed by this complex (oxidation or reduction of H₂) and how the diverse set of associated modules (HdrB, CdhA, SdhA, GcvH, and ion transporter) are regulated will require experimental work.

Searches using the genes encoding HdrB and [NiFe]-hydrogenase catalytic subunit revealed gene clusters with similar synteny to the ones encoding the Ehd and Ehe complexes in the methanogenic *Methanocellales* (Fig. 4C, G; denoted Drh) and in the predicted methanogenic Nezharchaeia (Fig. 4D, H; termed here Ehg) [8, 92]. Both gene clusters that encode the Drh and Ehg complexes retain the core structure of the [NiFe]-hydrogenase and HdrB genes, but co-located genes differ. Specifically, the Drh complex in *Methanocellales* lacks an ion antiporter subunit, which suggests that it is not involved in energy conservation via the

production of an ion gradient, but instead could be directly involved in the reduction of CoM-S-S-CoB coupled to H₂ oxidation [92]. The proposed Ehg gene cluster in Nezharchaeia MAGs is co-located with genes for a formate dehydrogenase subunit (FdhF), HdrA subunit, MvhD subunit, and an ion antiporter subunit. This suggests that oxidation of H₂, formate, or ferredoxin might be coupled to the direct reduction of CoM-S-S-CoB and the translocation of protons outside of the cell, thus conserving energy during their proposed hydrogenotrophic methanogenesis.

Phylogenetic analysis of the [NiFe]-hydrogenase catalytic subunit revealed that the Ehd, Ehe, and Drh complexes form a distinct cluster relative to other classified group 4 [NiFe]-hydrogenases. In contrast, the Ehg complex in Nezharchaeia forms a separate clade near a set of group 4g [NiFe]-hydrogenases (Fig. 4I). Additionally, JZ-Bin-30 encodes a second putative HdrB and membrane associated [NiFe]-hydrogenase complex that clusters with Bathyarchaeia and Methanomethylica sequences (Fig. 4I). This cluster was termed Ehd-like, due to the similarity in synteny to the Ehd complex in Methanomethylica, which lacks associated SdhA, CdhA, and GcvH subunits.

Importantly, these observations suggest that the strategy of coupling disulfide reductase activity to membrane bound [NiFe]-hydrogenases and ion translocation may be common in both methanogenic and non-methanogenic archaeal lineages. The apparent modular nature of these complexes may have allowed for diversification in substrate usage in the case of Culexarchaeia (succinate, CO) and Nezharchaeia (formate) for their respective metabolisms. Culturing representatives from the Culexarchaeia, Methanomethylica, or Nezharchaeia lineages would enable investigations into the function of these disulfide-interacting group 4 [NiFe]-hydrogenases in the metabolism of these organisms.

CONCLUSION

Here we report on a new archaeal class within the TACK superphylum, “*Candidatus* Culexarchaeia”, that is most closely related to the proposed methylotrophic and methanogenic lineage “*Ca.* Methanomethylica” (Verstraetearchaeota) [12]. In contrast to their closest relatives, Culexarchaeia encode the potential for non-methanogenic anaerobic methylotrophy but not methanogenesis. Furthermore, they encode the potential for a generalist lifestyle, with the capacity to use a diverse set of organic (sugars, lipids, proteins) and inorganic (H₂, CO, S⁰) substrates. Notably, the potential for anaerobic non-methanogenic methylotrophy and cyanophycin degradation, which to our current knowledge are not widespread among archaea, suggests that Culexarchaeia may be important in cycling these compounds in extreme environments and that these putative functions could be exploited in future cultivation attempts. The biogeographic distribution of terrestrial and marine Culexarchaeia indicates that they are found in high temperature (>50 °C) and circumneutral to slightly acidic (pH 5.4–7.8) environments. The capacity to metabolize many organic and inorganic substrates suggests that they could be important in the biogeochemical cycles of hydrogen, carbon, and sulfur within these diverse geothermal habitats, even at low relative abundances. The metabolic versatility encoded by Culexarchaeia could imply adaptations to changing nutrient conditions present in dynamic geothermal systems, because they could access a wide variety of compounds for their carbon and energy needs. Additionally, Culexarchaeia expand the diversity of cell division and cytoskeletal proteins in the TACK archaea, as they encode FtsZ-like, CdvBC, crenactin, and arcadin proteins. Future studies will need to determine how these diverse cell division and cytoskeletal proteins contribute to cell cycle and maintenance processes in Culexarchaeia, and could aid in understanding other lineages that similarly encode multiple division and cytoskeletal systems (e.g., Caldarchaeales (Aigarchaeota), Heimdallarchaeota, and Odinarchaeota).

Candidatus Culexarchaeum gen. nov.

Cu.lex.ar.chae'um N.L. neut. n. *Culex*, referring to the *Culex* Basin; N.L. neut. n. *archaeum*, an archaeon; N.L. neut. n. *Culexarchaeum*, archaeon of *Culex*, referring to the *Culex* Basin of Yellowstone National Park, where this lineage was discovered. The type species is *Candidatus Culexarchaeum yellowstonense*.

Candidatus Culexarchaeum yellowstonense sp. nov.

yel.low.ston.en'se N.L. neut. adj. *yellowstonense*, from Yellowstone National Park. This uncultured lineage is represented by bin YNP-LCB-024-027, recovered from an unnamed hot spring in the *Culex* Basin of Yellowstone National Park. The bin has an estimated completeness of 97.2% and a contamination of 0.93% and contains 16S rRNA, 23S rRNA and 5S rRNA genes.

Candidatus Culexarchaeum nevadense sp. nov.

ne.va.den'se N.L. neut. adj. *nevadense*, from Nevada. This uncultured lineage is represented by bin GBS-70-058, recovered from Great Boiling Springs in Nevada. The bin has an estimated completeness of 96.7% and a contamination of 0.07% and contains 16S rRNA, 23S rRNA, and 5S rRNA genes.

Candidatus Culexarchaeum jinzeense sp. nov.

jin.ze.en'se N.L. neut. adj. *jinzeense*, from Jinze. Represented by bin JZ-bin-30, recovered from a geothermal well in Jinze, Yunnan Province, China). The bin has an estimated completeness of 96.7%, a contamination of 0%, and contains 16S rRNA, 23S rRNA, and 5S rRNA genes. For a justification for the reclassification of this previously published bin [48], please see Supplementary Text.

Candidatus Culexmicrobiaceae fam. nov.

Cu.lex.mi.cro.bi.ace'ae. N.L. neut. n. *Culexmicrobium*, type genus of the family; L. -aceae ending to designate a family; N.L. fem. pl. n. *Culexmicrobiaceae*, the *Culexmicrobium* family. The description is the same as for *Candidatus Culexmicrobium* gen. nov.

Candidatus Culexmicrobium gen. nov.

Cu.lex.mi.cro.bi.ace'ae. N.L. neut. n. *Culex*, referring to the *Culex* Basin; N.L. neut. n. *microbium*, a microbe; N.L. neut. n. *Culexmicrobium*, microbe of *Culex*, referring to the *Culex* Basin of Yellowstone National Park, where this lineage was discovered. The type species is *Candidatus Culexmicrobium cathedralensis*.

Candidatus Culexmicrobium cathedralense sp. nov.

ca.the.dra.len'se N.L. neut. adj. *cathedralense*, from Cathedral Hill, a deep-sea hydrothermal vent in Guaymas Basin. This uncultured lineage is represented by bin GB-1867-05, recovered from deep-sea hydrothermal sediment in Guaymas Basin in the Gulf of California (i.e., Sea of Cortés). The bin has an estimated completeness of 99%, a contamination of 3.74%, and contains 16S rRNA, 23S rRNA and 5S rRNA genes.

Candidatus Culexmicrobium thermophilum sp. nov.

ther.mo.phil'um N.L. neut. adj. *thermophilum*, heat-loving. This uncultured lineage is represented by bin GB-1845-036, recovered from deep-sea hydrothermal sediment in Guaymas Basin in the Gulf of California (i.e., Sea of Cortés). The bin has an estimated completeness of 99%, a contamination of 3.74%, and contains 16S rRNA, 23S rRNA and 5S rRNA genes.

Candidatus Culexmicrobium profundum sp. nov.

pro.fund'um N.L. neut. adj. *profundum*, deep. Represented by bin GB-1867-035, recovered from deep-sea hydrothermal sediment in Guaymas Basin in the Gulf of California (i.e., Sea of Cortés). The bin has an estimated completeness of 96.7%, a contamination of 7.79%, and contains a 5S rRNA gene.

DATA AVAILABILITY

The raw metagenomes used to recover MAGs of *Culexarchaeia* representatives are publicly available through the JGI IMG-MER database under accession numbers 3300029977 (YNP-LCB-024), 3300028675 (YNP-LCB-003), 3300005860 (YNP-WB), 3300020139 (GBS), 3300021469 (GB-1845), and 3300021472 (GB-1867). The nine *Culexarchaeia* MAGs newly recovered in this study are available in NCBI under BioProject ID PRJNA819097. The JZ-Bin-30 MAG is publicly available through the JGI IMG-MER database accession number Ga0181710.

REFERENCES

- Adam PS, Borrel G, Brochier-Armanet C, Gribaldo S. The growing tree of Archaea: new perspectives on their diversity, evolution and ecology. *ISME J.* 2017;11:2407–25.
- Baker BJ, De Anda V, Seitz KW, Dombrowski N, Santoro AE, Lloyd KG. Diversity, ecology and evolution of Archaea. *Nat Microbiol.* 2020;5:887–900.
- Huber H, Hohn MJ, Rachel R, Fuchs T, Wimmer VC, Stetter KO. A new phylum of Archaea represented by a nanosized hyperthermophilic symbiont. *Nature.* 2002;417:63–7.
- Barns SM, Delwiche CF, Palmer JD, Pace NR. Perspectives on archaeal diversity, thermophily and monophyly from environmental rRNA sequences. *Proc Natl Acad Sci.* 1996;93:9188–93.
- Kozubal MA, Romine M, deM Jennings R, Jay ZJ, Tringe SG, Rusch DB, et al. Geoarchaeota: a new candidate phylum in the Archaea from high-temperature acidic iron mats in Yellowstone National Park. *ISME J.* 2013;7:622–34.
- Zaremba-Niedzwiedzka K, Caceres EF, Saw JH, Bäckström D, Juzokaite L, Vancaester E, et al. Asgard archaea illuminate the origin of eukaryotic cellular complexity. *Nature.* 2017;541:353–8.
- Jay ZJ, Beam JP, Dlakić M, Rusch DB, Kozubal MA, Inskeep WP. Marsarchaeota are an aerobic archaeal lineage abundant in geothermal iron oxide microbial mats. *Nat Microbiol.* 2018;3:732–40.
- Wang Y, Wegener G, Hou J, Wang F, Xiao X. Expanding anaerobic alkane metabolism in the domain of Archaea. *Nat Microbiol.* 2019;4:595–602.
- De Anda V, Chen L-X, Dombrowski N, Hua Z-S, Jiang H-C, Banfield JF, et al. Brockarchaeota, a novel archaeal phylum with unique and versatile carbon cycling pathways. *Nat Commun.* 2021;12:1–12.
- Offre P, Spang A, Schleper C. Archaea in biogeochemical cycles. *Ann Rev Microbiol.* 2013;67:437–57.
- Spang A, Caceres EF, Ettema TJ. Genomic exploration of the diversity, ecology, and evolution of the archaeal domain of life. *Science.* 2017;357:eaa3883.
- Vanwonterghem I, Evans PN, Parks DH, Jensen PD, Woodcroft BJ, Hugenholtz P, et al. Methylothermophilic methanogenesis discovered in the archaeal phylum *Verstraearchaeota*. *Nature Microbiol.* 2016;1:1–9.
- Evans PN, Parks DH, Chadwick GL, Robbins SJ, Orphan VJ, Golding SD, et al. Methane metabolism in the archaeal phylum *Bathyarchaeota* revealed by genome-centric metagenomics. *Science.* 2015;350:434–8.
- McKay LJ, Dlakić M, Fields MW, Delmont TO, Eren AM, Jay ZJ, et al. Co-occurring genomic capacity for anaerobic methane and dissimilatory sulfur metabolisms discovered in the *Korarchaeota*. *Nat Microbiol.* 2019;4:614–22.
- Borrel G, Adam PS, McKay LJ, Chen L-X, Sierra-García IN, Sieber CM, et al. Wide diversity of methane and short-chain alkane metabolisms in uncultured archaea. *Nat Microbiol.* 2019;4:603–13.
- Lloyd KG, Steen AD, Ladau J, Yin J, Crosby L. Phylogenetically novel uncultured microbial cells dominate earth microbiomes. *MSystems.* 2018;3:e00055–18.
- Nurk S, Meleshko D, Korobeynikov A, Pevzner PA. metaSPAdes: a new versatile metagenomic assembler. *Genome Res.* 2017;27:824–34.
- Thomas SC, Tamadonfar KO, Seymour CO, Lai D, Dodsworth JA, Murugapiran SK, et al. Position-specific metabolic probing and metagenomics of microbial communities reveal conserved central carbon metabolic network activities at high temperatures. *Front Microbiol.* 2019;10:1427.
- Chen I-MA, Chu K, Palaniappan K, Pillay M, Ratner A, Huang J, et al. IMG/M v. 5.0: an integrated data management and comparative analysis system for microbial genomes and microbiomes. *Nucleic acids Res.* 2019;47:D666–D77.
- Wu Y-W, Tang Y-H, Tringe SG, Simmons BA, Singer SW. MaxBin: an automated binning method to recover individual genomes from metagenomes using an expectation-maximization algorithm. *Microbiome.* 2014;2:1–18.
- Alneberg J, Bjarnason BS, De Bruijn I, Schirmer M, Quick J, Ijaz UZ, et al. Binning metagenomic contigs by coverage and composition. *Nat Methods.* 2014;11:144–6.
- Kang DD, Li F, Kirton E, Thomas A, Egan R, An H, et al. MetaBAT 2: an adaptive binning algorithm for robust and efficient genome reconstruction from metagenome assemblies. *PeerJ.* 2019;7:e7359.
- Miller IJ, Rees ER, Ross J, Miller I, Baxa J, Lopera J, et al. Autometa: automated extraction of microbial genomes from individual shotgun metagenomes. *Nucleic Acids Res.* 2019;47:e57–e.
- Sieber CM, Probst AJ, Sharrar A, Thomas BC, Hess M, Tringe SG, et al. Recovery of genomes from metagenomes via a dereplication, aggregation and scoring strategy. *Nat Microbiol.* 2018;3:836–43.
- Hua Z-S, Qu Y-N, Zhu Q, Zhou E-M, Qi Y-L, Yin Y-R, et al. Genomic inference of the metabolism and evolution of the archaeal phylum *Aigarchaeota*. *Nat Commun.* 2018;9:1–11.
- Hua Z-S, Wang Y-L, Evans PN, Qu Y-N, Goh KM, Rao Y-Z, et al. Insights into the ecological roles and evolution of methyl-coenzyme M reductase-containing hot spring Archaea. *Nat Commun.* 2019;10:1–11.
- Parks DH, Imelfort M, Skennerton CT, Hugenholtz P, Tyson GW. CheckM: assessing the quality of microbial genomes recovered from isolates, single cells, and metagenomes. *Genome Res.* 2015;25:1043–55.

28. Chan PP, Lowe TM. tRNAscan-SE: Searching for tRNA Genes in Genomic Sequences. *Methods Mol Biol.* 2019;1962:1–14.
29. Li G, Rabe KS, Nielsen J, Engqvist MK. Machine learning applied to predicting microorganism growth temperatures and enzyme catalytic optima. *ACS Synthetic Biol.* 2019;8:1411–20.
30. Inskeep W, Ackerman G, Taylor W, Kozubal M, Korf S, Macur R. On the energetics of chemolithotrophy in nonequilibrium systems: case studies of geothermal springs in Yellowstone National Park. *Geobiology.* 2005;3:297–317.
31. Nawrocki EP, Kolbe DL, Eddy SR. Infernal 1.0: inference of RNA alignments. *Bioinformatics.* 2009;25:1335–7.
32. Minh BQ, Schmidt HA, Chernomor O, Schrempf D, Woodhams MD, Von Haeseler A, et al. IQ-TREE 2: New models and efficient methods for phylogenetic inference in the genomic era. *Mol Biol Evol.* 2020;37:1530–4.
33. Edgar RC. MUSCLE: multiple sequence alignment with high accuracy and high throughput. *Nucleic Acids Res.* 2004;32:1792–7.
34. Capella-Gutiérrez S, Silla-Martínez JM, Gabaldón T. trimAl: a tool for automated alignment trimming in large-scale phylogenetic analyses. *Bioinformatics.* 2009;25:1972–3.
35. Søndergaard D, Pedersen CN, Greening C. HydDB: a web tool for hydrogenase classification and analysis. *Sci Rep.* 2016;6:1–8.
36. Liao Y, Ithurbe S, Evenhuis C, Löwe J, Duggin IG. Cell division in the archaeon *Haloferax volcanii* relies on two FtsZ proteins with distinct functions in division ring assembly and constriction. *Nat Microbiol.* 2021;6:594–605.
37. Duggin IG, Aylett CH, Walsh JC, Michie KA, Wang Q, Turnbull L, et al. CetZ tubulin-like proteins control archaeal cell shape. *Nature.* 2015;519:362–5.
38. Makarova KS, Koonin EV. Two new families of the FtsZ-tubulin protein superfamily implicated in membrane remodeling in diverse bacteria and archaea. *Biol Direct.* 2010;5:1–9.
39. Lu S, Wang J, Chitsaz F, Derbyshire MK, Geer RC, Gonzales NR, et al. CDD/SPARCLE: the conserved domain database in 2020. *Nucleic Acids Res.* 2020;48:D265–D8.
40. Jones P, Binns D, Chang H-Y, Fraser M, Li W, McAnulla C, et al. InterProScan 5: genome-scale protein function classification. *Bioinformatics.* 2014;30:1236–40.
41. Krogh A, Larsson B, Von Heijne G, Sonnhammer EL. Predicting transmembrane protein topology with a hidden Markov model: application to complete genomes. *J Mol Biol.* 2001;305:567–80.
42. Spang A, Hatzepichler R, Brochier-Armanet C, Rattei T, Tischler P, Spieck E, et al. Distinct gene set in two different lineages of ammonia-oxidizing archaea supports the phylum Thaumarchaeota. *Trends Microbiol.* 2010;18:331–40.
43. Brochier-Armanet C, Forterre P, Gribaldo S. Phylogeny and evolution of the Archaea: one hundred genomes later. *Curr Opin Microbiol.* 2011;14:274–81.
44. Guy L, Ettema TJ. The archaeal 'TACK' superphylum and the origin of eukaryotes. *Trends Microbiol.* 2011;19:580–7.
45. Makarova KS, Wolf YI, Koonin EV. Archaeal clusters of orthologous genes (arCOGs): an update and application for analysis of shared features between Thermococcales, Methanococcales, and Methanobacteriales. *Life.* 2015;5:818–40.
46. Eddy SR. Accelerated profile HMM searches. *PLoS Comput Biol.* 2011;7:e1002195. <https://doi.org/10.1371/journal.pcbi.1002195>.
47. Rinke C, Chuvochina M, Mussig AJ, Chaumeil P-A, Waite DW, Davin AA, et al. A standardized archaeal taxonomy for the Genome Taxonomy Database. *Nat Microbiol.* 2021;6:946–59.
48. Berghuis BA, Yu FB, Schulz F, Blainey PC, Woyke T, Quake SR. Hydrogenotrophic methanogenesis in archaeal phylum Verstraetearchaeota reveals the shared ancestry of all methanogens. *Proc Natl Acad Sci.* 2019;116:5037–44.
49. Teske A, De Beer D, McKay LJ, Tivey MK, Biddle JF, Hoer D, et al. The Guaymas Basin hiking guide to hydrothermal mounds, chimneys, and microbial mats: Complex seafloor expressions of subsurface hydrothermal circulation. *Front Microbiol.* 2016;7:75.
50. Forterre P. A hot story from comparative genomics: reverse gyrase is the only hyperthermophile-specific protein. *Trends Genetics.* 2002;18:236–7.
51. Lipscomb GL, Hahn EM, Crowley AT, Michael W, Adams W. Reverse gyrase is essential for microbial growth at 95 °C. *Extremophiles.* 2017;21:603.
52. Pende N, Sogues A, Megrian D, Sartori-Rupp A, England P, Palabikyan H, et al. SepF is the FtsZ anchor in archaea, with features of an ancestral cell division system. *Nat Commun.* 2021;12:1–13.
53. Makarova KS, Yutin N, Bell SD, Koonin EV. Evolution of diverse cell division and vesicle formation systems in Archaea. *Nat Rev Microbiol.* 2010;8:731–41.
54. Ettema TJ, Lindås AC, Bernander R. An actin-based cytoskeleton in archaea. *Mol Microbiol.* 2011;80:1052–61.
55. Stairs CW, Ettema TJ. The archaeal roots of the eukaryotic dynamic actin cytoskeleton. *Curr Biol.* 2020;30:R521–R6.
56. Bernander R, Lind AE, Ettema TJ. An archaeal origin for the actin cytoskeleton: implications for eukaryogenesis. *Commun Integr Biol.* 2011;4:664–7.
57. Kelly RM, Adams MW. Metabolism in hyperthermophilic microorganisms. *Antonie Van Leeuwenhoek.* 1994;66:247–70.
58. Musfeldt M, Schönheit P. Novel type of ADP-forming acetyl coenzyme A synthetase in hyperthermophilic archaea: heterologous expression and characterization of isoenzymes from the sulfate reducer *Archaeoglobus fulgidus* and the methanogen *Methanococcus jannaschii*. *J Bacteriol.* 2002;184:636–44.
59. Ma K, Hutchins A, Sung S-JS, Adams MW. Pyruvate ferredoxin oxidoreductase from the hyperthermophilic archaeon, *Pyrococcus furiosus*, functions as a CoA-dependent pyruvate decarboxylase. *Proc Natl Acad Sci.* 1997;94:9608–13.
60. Nissen LS, Basen M. The emerging role of aldehyde: ferredoxin oxidoreductases in microbially-catalyzed alcohol production. *J Biotechnol.* 2019;306:105–17.
61. van den Ban EC, Willemen HM, Wassink H, Laane C, Haaker H. Bioreduction of carboxylic acids by *Pyrococcus furiosus* in batch cultures. *Enzyme Microb Technol.* 1999;25:251–7.
62. Sapra R, Bagramyan K, Adams MW. A simple energy-conserving system: proton reduction coupled to proton translocation. *Proc Natl Acad Sci.* 2003;100:7545–50.
63. Richter R, Hejazi M, Kraft R, Ziegler K, Lockow W. Cyanophycinase, a peptidase degrading the cyanobacterial reserve material multi-L-arginyl-poly-L-aspartic acid (cyanophycin) Molecular cloning of the gene of *Synechocystis* sp. PCC 6803, expression in *Escherichia coli*, and biochemical characterization of the purified enzyme. *Eur J Biochem.* 1999;263:163–9.
64. Fuser G, Steinbüchel A. Analysis of genome sequences for genes of cyanophycin metabolism: identifying putative cyanophycin metabolizing prokaryotes. *Macromol Biosci.* 2007;7:278–96.
65. Maghnooui A, de Sousa Cabral TF, Stalon V, Vander Wauwen C. The arcABDC gene cluster, encoding the arginine deiminase pathway of *Bacillus licheniformis*, and its activation by the arginine repressor argR. *J Bacteriol.* 1998;180:6468–75.
66. Wong HL, White RA, Visscher PT, Charlesworth JC, Vázquez-Campos X, Burns BP. Disentangling the drivers of functional complexity at the metagenomic level in Shark Bay microbial mat microbiomes. *ISME J.* 2018;12:2619–39.
67. Wagner T, Ermiler U, Shima S. MtrA of the sodium ion pumping methyltransferase binds cobalamin in a unique mode. *Sci Rep.* 2016;6:1–10.
68. Ticak T, Kountz DJ, Girosky KE, Krzycki JA, Ferguson DJ. A nonpyrrolysine member of the widely distributed trimethylamine methyltransferase family is a glycine betaine methyltransferase. *Proc Natl Acad Sci.* 2014;111:E4668–E76.
69. Kountz DJ, Behrman EJ, Zhang L, Krzycki JA. MtcB, a member of the MttB superfamily from the human gut acetogen *Eubacterium limosum*, is a cobalamin-dependent carnitine demethylase. *J Biol Chem.* 2020;295:11971–81.
70. Adam PS, Borrel G, Gribaldo S. An archaeal origin of the Wood-Ljungdahl H4MPT branch and the emergence of bacterial methylation. *Nat Microbiol.* 2019;4:2155–63.
71. Dibrova DV, Galperin MY, Mulikidjanian AY. Phylogenomic reconstruction of archaeal fatty acid metabolism. *Environ Microbiol.* 2014;16:907–18.
72. Garcia Costas AM, Poudel S, Miller A-F, Schut GJ, Ledbetter RN, Fixen KR, et al. Defining electron bifurcation in the electron-transferring flavoprotein family. *J Bacteriol.* 2017;199:e00440–17.
73. Beam JP, Jay ZJ, Schmid MC, Rusch DB, Romine MF, de M, et al. Ecophysiology of an uncultivated lineage of Aigarchaeota from an oxidic, hot spring filamentous 'streamer' community. *ISME J.* 2016;10:210–24.
74. Dobbek H, Gremer L, Kiefersauer R, Huber R, Meyer O. Catalysis at a dinuclear [CuSmO(O)OH] cluster in a CO dehydrogenase resolved at 1.1-Å resolution. *Proc Natl Acad Sci.* 2002;99:15971–6.
75. Cordero PR, Bayly K, Leung PM, Huang C, Islam ZF, Schittenhelm RB, et al. Atmospheric carbon monoxide oxidation is a widespread mechanism supporting microbial survival. *ISME J.* 2019;13:2868–81.
76. Bräsen C, Esser D, Rauch B, Siebers B. Carbohydrate metabolism in Archaea: current insights into unusual enzymes and pathways and their regulation. *Microbiol Mol Biol Rev.* 2014;78:89–175.
77. Say RF, Fuchs G. Fructose 1, 6-bisphosphate aldolase/phosphatase may be an ancestral gluconeogenic enzyme. *Nature.* 2010;464:1077–81.
78. Kato N, Yurimoto H, Thauer RK. The physiological role of the ribulose monophosphate pathway in bacteria and archaea. *Biosci Biotechnol Biochem.* 2006;70:10–21.
79. Müller V, Chowdhury NP, Basen M. Electron bifurcation: a long-hidden energy-coupling mechanism. *Ann Rev Microbiol.* 2018;72:331–53.
80. Buckel W, Thauer RK. Flavin-based electron bifurcation, a new mechanism of biological energy coupling. *Chem Rev.* 2018;118:3862–86.
81. Poudel S, Dunham EC, Lindsay MR, Amenabar MJ, Fones EM, Colman DR, et al. Origin and evolution of flavin-based electron bifurcating enzymes. *Front Microbiol.* 2018;9:1762.
82. Wagner T, Koch J, Ermiler U, Shima S. Methanogenic heterodisulfide reductase (HdrABC-MvhAGD) uses two noncubane [4Fe-4S] clusters for reduction. *Science.* 2017;357:699–703.
83. Arshad A, Speth DR, de Graaf RM, Op den Camp HJ, Jetten MS, Welte CU. A metagenomics-based metabolic model of nitrate-dependent anaerobic oxidation of methane by Methanoperedens-like archaea. *Front Microbiol.* 2015;6:1423.
84. Nguyen DM, Schut GJ, Zadvornyy OA, Tokmina-Lukaszewska M, Poudel S, Lipscomb GL, et al. Two functionally distinct NADP⁺-dependent ferredoxin

- oxidoreductases maintain the primary redox balance of *Pyrococcus furiosus*. *J Biol Chem*. 2017;292:14603–16.
85. Ma K, Schicho RN, Kelly RM, Adams M. Hydrogenase of the hyperthermophile *Pyrococcus furiosus* is an elemental sulfur reductase or sulfhydrogenase: evidence for a sulfur-reducing hydrogenase ancestor. *Proc Natl Acad Sci*. 1993;90:5341–4.
 86. Ma K, Weiss R, Adams MW. Characterization of hydrogenase II from the hyperthermophilic archaeon *Pyrococcus furiosus* and assessment of its role in sulfur reduction. *J Bacteriol*. 2000;182:1864–71.
 87. Yan Z, Wang M, Ferry JG. A ferredoxin-and F420H₂-dependent, electron-bifurcating, heterodisulfide reductase with homologs in the domains bacteria and archaea. *MBio*. 2017;8:e02285–16.
 88. LaRowe DE, Amend JP. The energetics of fermentation in natural settings. *Geomicrobiol J*. 2019;36:492–505.
 89. Shock EL, Holland M, Meyer-Dombard D, Amend JP. Geochemical sources of energy for microbial metabolism in hydrothermal ecosystems: Obsidian Pool, Yellowstone National Park. *Geotherm Biol Geochem Yellowstone Natl Park*. 2005;1:95–112.
 90. Cao X, Zhu L, Song X, Hu Z, Cronan JE. Protein moonlighting elucidates the essential human pathway catalyzing lipoic acid assembly on its cognate enzymes. *Proc Natl Acad Sci*. 2018;115:E7063–E72.
 91. Tezuka T, Ohnishi Y. Two glycine riboswitches activate the glycine cleavage system essential for glycine detoxification in *Streptomyces griseus*. *J Bacteriol*. 2014;196:1369–76.
 92. Lyu Z, Lu Y. Comparative genomics of three *M* ethanocellales strains reveal novel taxonomic and metabolic features. *Environ Microbiol Rep*. 2015;7:526–37.
 93. Wang Y, Wegener G, Williams TA, Xie R, Hou J, Tian C, et al. A methylotrophic origin of methanogenesis and early divergence of anaerobic multicarbon alkane metabolism. *Sci Adv*. 2021;7:eabj1453.
 94. Evans PN, Boyd JA, Leu AO, Woodcroft BJ, Parks DH, Hugenholtz P, et al. An evolving view of methane metabolism in the Archaea. *Nat Rev Microbiol*. 2019;17:219–32.
 95. Zinke LA, Evans PN, Santos-Medellín C, Schroeder AL, Parks DH, Varner RK, et al. Evidence for non-methanogenic metabolisms in globally distributed archaeal clades basal to the Methanomassiliicoccales. *Environ Microbiol*. 2021;23:340–57.
 96. Chuvochina M, Rinke C, Parks DH, Rappé MS, Tyson GW, Yilmaz P, et al. The importance of designating type material for uncultured taxa. *System Appl Microbiol*. 2019;42:15–21.
 97. Vaughan RG, Heasler H, Jaworowski C, Lowenstern JB, Keszthelyi LP. Provisional maps of thermal areas in Yellowstone National Park, based on satellite thermal infrared imaging and field observations. *US Geol Surv Sci Investig Rep*. 2014;5137:22.

ACKNOWLEDGEMENTS

We thank Drs. Barbara MacGregor, William Inskeep and Mensur Dlakić, as well as Brian Hedlund and Ramunas Stepanauskas for permitting use of their metagenomes and for providing metadata information for Guaymas Basin sediments, Washburn Hot Springs, and Great Boiling Spring, respectively. We acknowledge Christine Gobrogge at Montana State University's Environmental Analytical Laboratory for assisting with geochemical analyses. We further thank Drs. Brian Hedlund and Marike Palmer for discussing nomenclatural types and taxonomic naming and Grayson Chadwick for helpful comments on the manuscript. This study was funded through a NASA Exobiology program award to RH (80NSSC19K1633). AJK and ML were supported in part by the Thermal Biology Institute and Montana State University's Vice President's

Office of Research, Economic Development and Graduate Education. VK was supported in part by a grant from the W.M. Keck Foundation. A portion of this research was performed under the Facilities Integrating Collaborations for User Science (FICUS) program (proposal: 10.46936/fics.proj.2017.49972/6000002) and used resources at the DOE Joint Genome Institute (<https://ror.org/04xm1d337>), which is a DOE Office of Science User Facility operated under Contract No. DE-AC02-05CH11231. We thank the US National Park Service, in particular Annie Carlson at the Yellowstone Center for Resources, for permitting work in YNP under permit number YELL-SCI-8010. NASA Exobiology 80NSSC19K1633.

AUTHOR CONTRIBUTIONS

AJK, ZJJ, and RH designed the research. MML and RH collected molecular and geochemical samples from YNP hot springs. AJK and ZJJ processed metagenome data, evaluated the MAGs, and performed phylogenomic and 16S rRNA analyses. AJK reconstructed the metabolic potential of *Culexarchaea*, performed the phylogenetic analyses of individual proteins, and ran FISH experiments. VK provided useful discussion and contributed to assessing metabolic potential. AJK and RH wrote the manuscript, which was edited by all authors.

COMPETING INTERESTS

The authors declare no competing interests.

ADDITIONAL INFORMATION

Supplementary information The online version contains supplementary material available at <https://doi.org/10.1038/s43705-022-00175-8>.

Correspondence and requests for materials should be addressed to Roland Hatzenpichler.

Reprints and permission information is available at <http://www.nature.com/reprints>

Publisher's note Springer Nature remains neutral with regard to jurisdictional claims in published maps and institutional affiliations.



Open Access This article is licensed under a Creative Commons Attribution 4.0 International License, which permits use, sharing, adaptation, distribution and reproduction in any medium or format, as long as you give appropriate credit to the original author(s) and the source, provide a link to the Creative Commons license, and indicate if changes were made. The images or other third party material in this article are included in the article's Creative Commons license, unless indicated otherwise in a credit line to the material. If material is not included in the article's Creative Commons license and your intended use is not permitted by statutory regulation or exceeds the permitted use, you will need to obtain permission directly from the copyright holder. To view a copy of this license, visit <http://creativecommons.org/licenses/by/4.0/>.

© The Author(s) 2022

Supplementary Information

for

Culexarchaeia, a novel archaeal class of anaerobic generalists inhabiting geothermal environments

Anthony J. Kohtz, Zackary J. Jay, Mackenzie Lynes, Viola Krukenberg, Roland Hatzenpichler

Supplementary Files

File Name: Supplemental Files 1-8 (Excel file)

Supplementary File 1: Lists of single copy marker genes, genomes, and genome identifiers used in the phylogenomic analysis shown in Figure 1A and Supplementary Figure 1.

Supplementary File 2: Presence-absence patterns for individual genomes, with genes involved in central information-processing machinery.

Supplementary File 3: Full list of genes found in Culexarchaeia MAGs that were used to construct Figure 3.

Supplementary File 4: Full list of abbreviations used in Figure 3.

Supplementary File 5: Full list of IMG or NCBI accessions for the [NiFe] hydrogenase complexes depicted in Figure 4.

Supplementary File 6: Presence and absence of methanogenesis marker proteins in Culexarchaeia and Methanomethylica (Verstraetearchaeota) MAGs.

Supplementary File 7: Metadata and geochemical data for YNP sites LCB-003 and LCB-024.

Supplementary File 8: Metadata for Culexarchaeia 16S rRNA genes in NCBI and IMG databases.

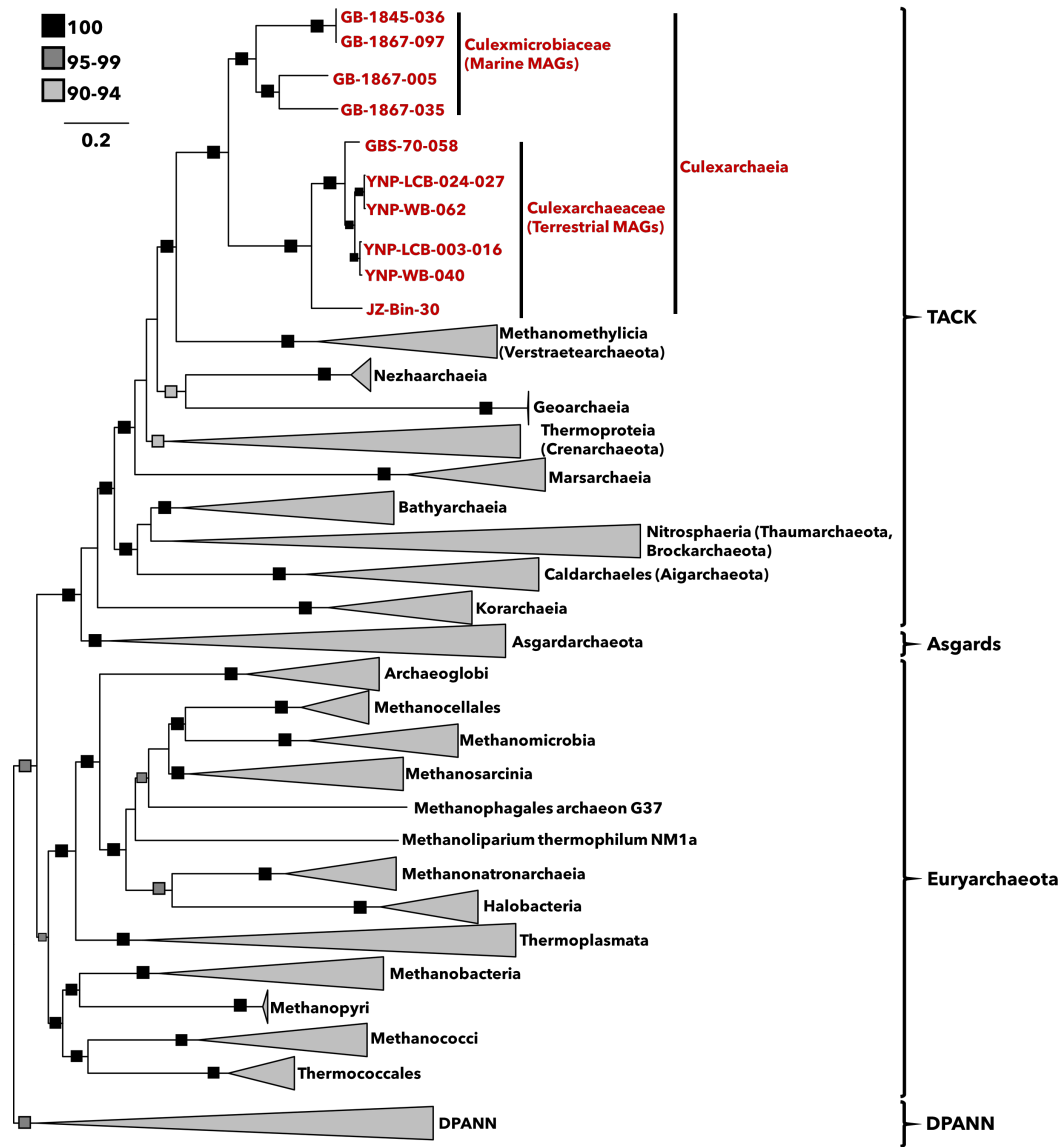
Supplementary Table 1 Temperature profiles recorded by Alvin’s heat flow probe on December 24th, 2016, during dive 4872. This table illustrates the dynamics of the hydrothermal vent field in Guaymas Basin, which makes an exact determination of the temperature at time of sampling hard. To ensure stable placement of the temperature probe, the probe’s disk had to be buried 2-3 cm in the sediment. The sediment sample from which the metagenome was retrieved was taken approximately 40-60 and 30-50 minutes after temperature profiles 1 and 2 were obtained, respectively. To not interfere with the integrity of the sample, the temperatures were taken 1-2 meters away from where the eventual sample was taken. The sample was collected from approximately half-way between where the two temperature profiles were taken. Geolocation of sample: 27° 00.684 N, 111° 24.266 W. Water depth: 2000 m. The temperatures most closely reflecting the *in situ* temperature range at the time of sampling are highlighted in bold (53.2 and 83.2 °C).

	Heat-flow probe location 1		Heat-flow probe location 2		
	Time 16:33	Time 16:36	Time 16:44	Time 16:47	Time 16:50
Temp. 1 (7-8 cm)	76.4 °C	83.2 °C	38.6 °C	50.7 °C	53.2 °C
Temp. 2 (~17 cm)	98.3 °C	101.8 °C	58.4 °C	71.1 °C	73.3 °C
Temp. 3 (~27 cm)	104.2 °C	105.6 °C	74.9 °C	81.8 °C	82.8 °C
Temp. 4 (~37 cm)	107.4 °C	108.1 °C	88.2 °C	92.1 °C	93.1 °C
Temp. 5 (~47 cm)	107.2 °C	107.7 °C	98.1 °C	100.1 °C	101.3 °C

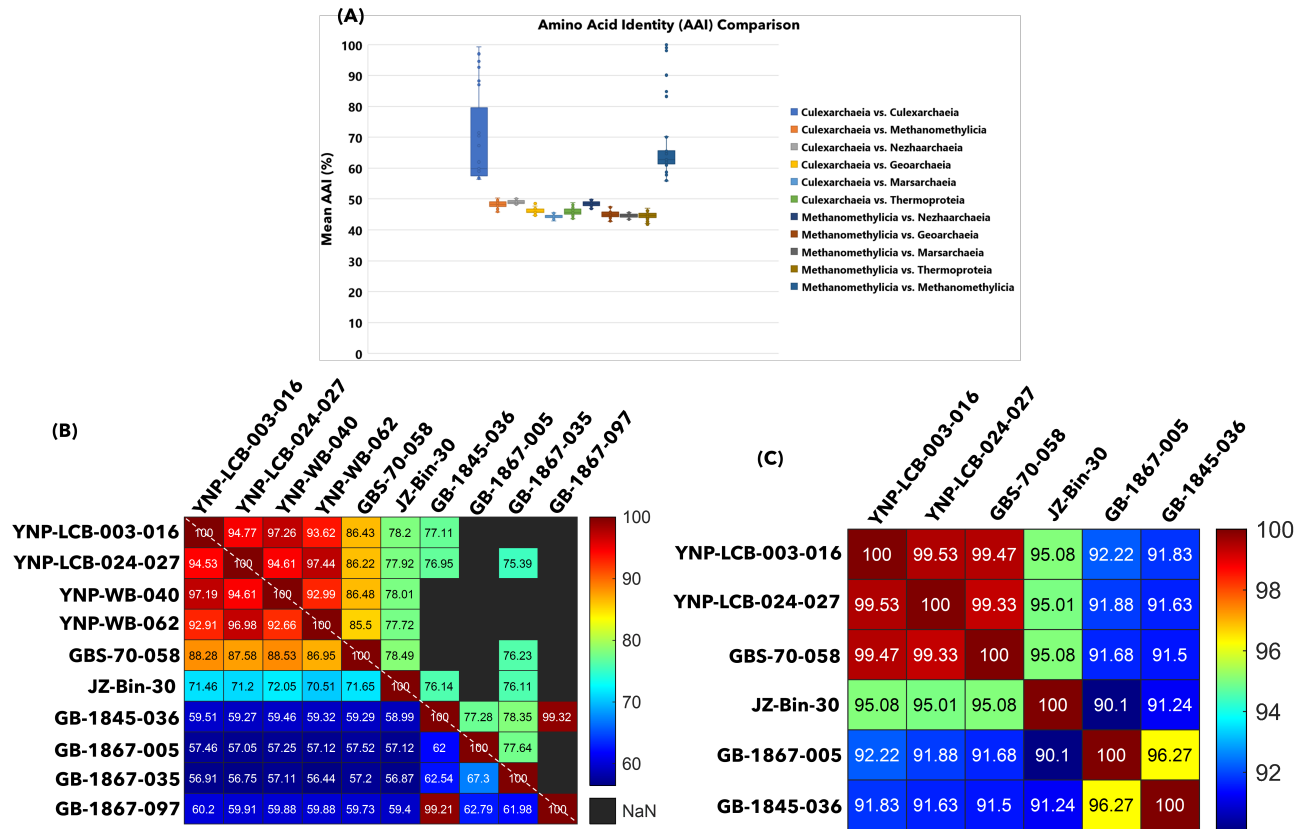
Supplementary Table 2 Proposed naming scheme for the Culexarchaeia MAGs used in this study. Family, genus, and species designations were decided by considering our phylogenomic tree (Figure 1A), pairwise 16S rRNA gene nucleotide identities, and pairwise MAG AAI values. *, indicates MAG ID used to designate type species.

Phylum	Class	Order	Family	Genus	Species	MAG ID
Culexarchaeota (NCBI) / Thermoproteota (GTDB)	Culexarchaeia	Culexarchaeles	Culexarchaeaceae	Culexarchaeum	yellowstonense	YNP-LCB-24-027 *
						YNP-LCB-3-016
						YNP-WB-040
						YNP-WB-062
					jinzeense	JZ-Bin-30 *
			nevadense	GBS-70-058 *		
			Culexmicrobiacea e	Culexmicrobium	cathedralense	GB-1867-005 *
					profundum	GB-1867-035 *
					thermophilum	GB-1845-036 *
						GB-1867-097

Supplementary figures



Supplementary Figure 1 Phylogenomic tree of Culexarchaeia MAGs and reference archaeal genomes. Maximum-likelihood tree, inferred with IQtree and the best-fit LG+C60+F+G model, using a concatenated set of 46 conserved ribosomal proteins (Supplementary File 1). Ultrafast bootstrap support values of 100, 95-99, and 90-94 are indicated with black, dark gray, and light gray squares, respectively.

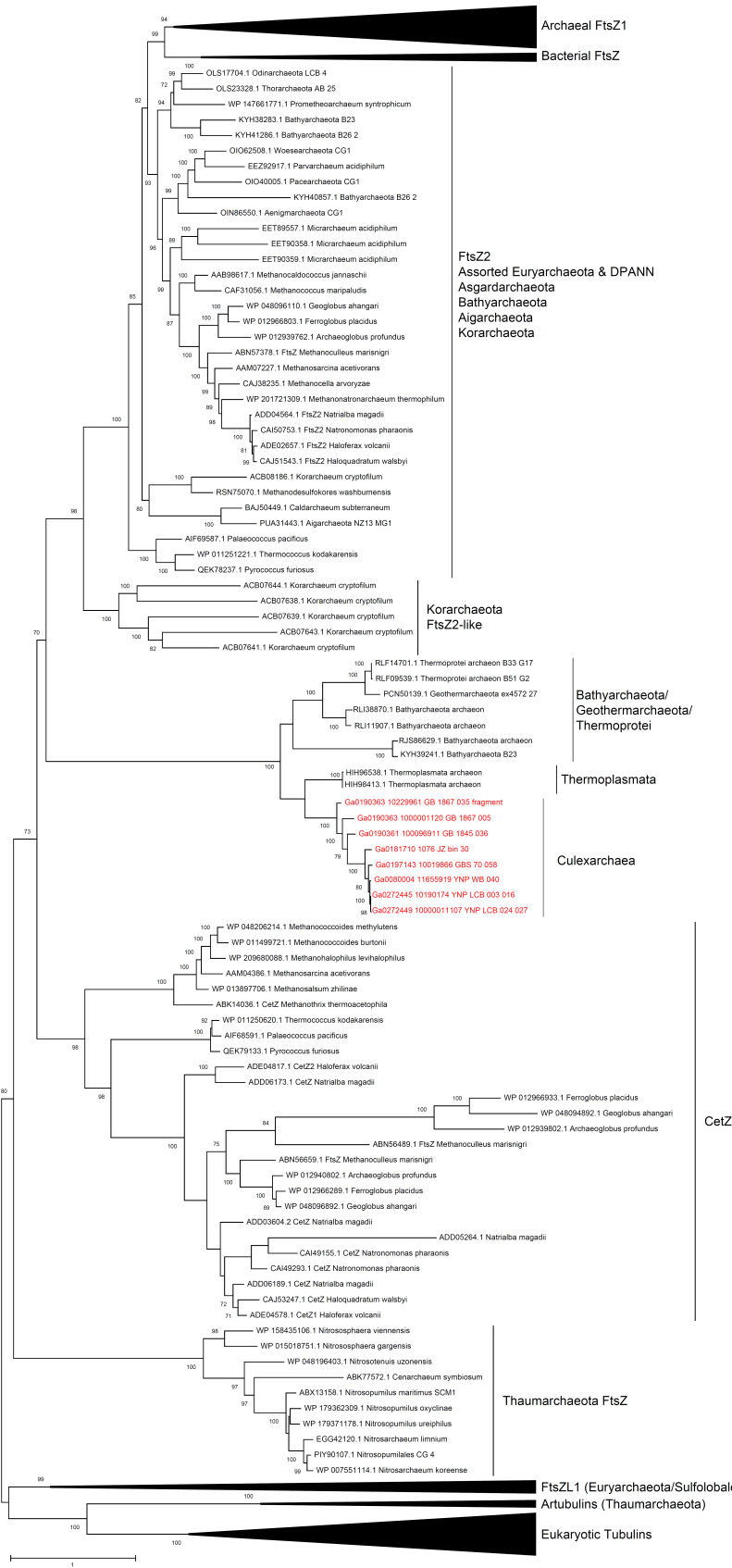


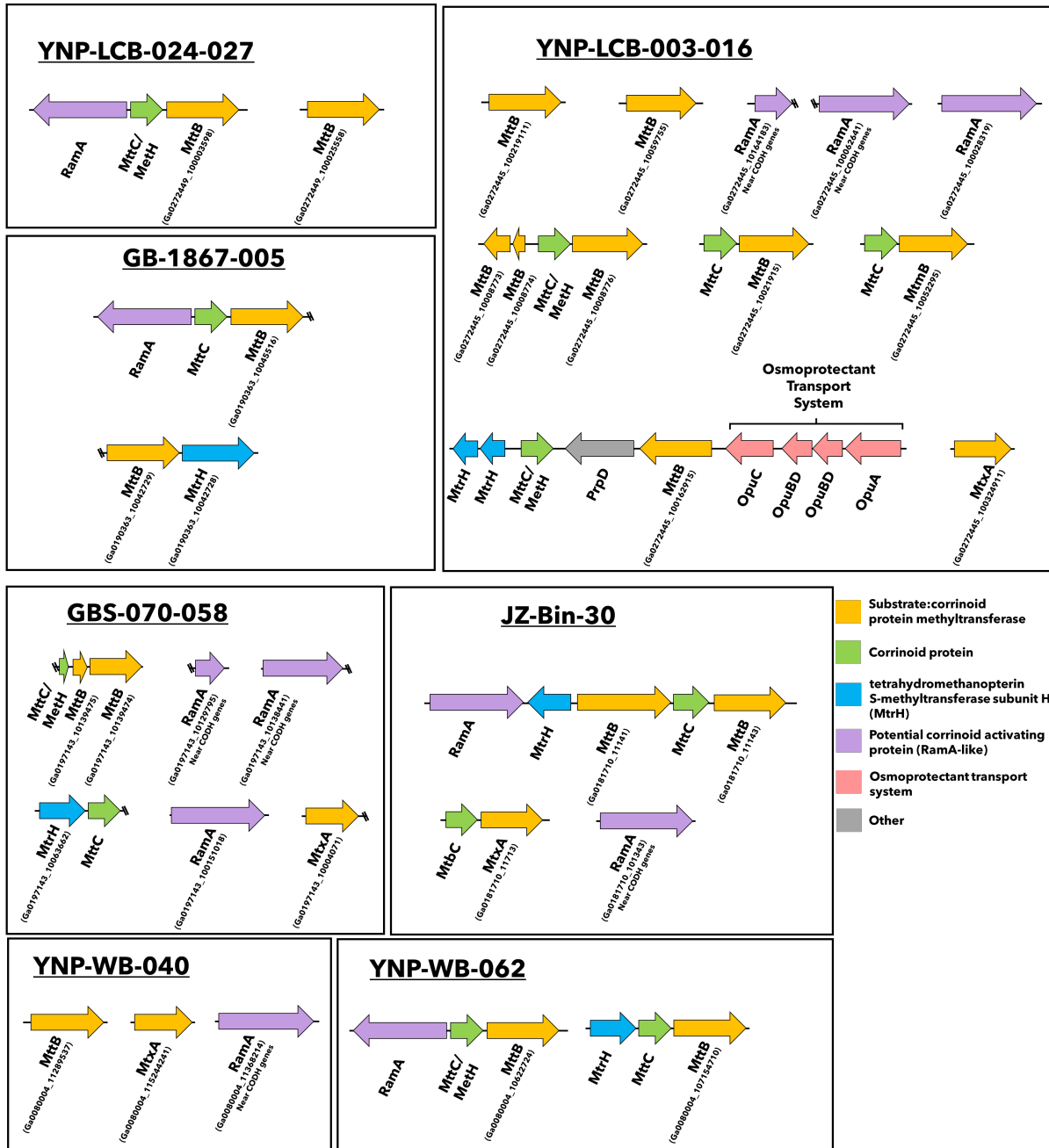
Supplementary Figure 2 Amino acid identities (AAI) of Culexarchaeia and major TACK lineages. Intra-clade AAI, ANI, and 16S rRNA gene percent identity of Culexarchaeia. (A) Analysis shows that the average AAI between TACK classes is below 50%, consistent with the designation of Culexarchaeia as a class level lineage within the TACK superphylum. Thick bar, median; first and third quartile, upper and lower bounds of the box, respectively. Upper and lower whiskers extend to the highest and lowest values within 1.5x of the interquartile range, respectively. **(B)** Intra-clade AAI and ANI of Culexarchaeia. Values above and below the dashed white line represent ANI and AAI values, respectively. AAI values were calculated with compareM and ANI values were calculated with fastANI. **(C)** Pairwise % identity of Culexarchaeia 16S rRNA gene sequences calculated by BLASTn.

Supplementary Figure 3

Maximum likelihood phylogeny of tubulin superfamily proteins.

Amino acid sequences were aligned using Mafft-LINSi and trimmed with a 70% gap threshold using trimal. Tree was constructed with IQtree2 and the best fit model LG+R5. Ultrafast bootstrap support values above 70 are indicated at each node, and values below 70 are not displayed. Culexarchaeia FtsZ-like sequences are highlighted in red.





Supplementary Figure 4 Organization of *Culexarchaemia* methyltransferase genes. The color of the arrows corresponds to the predicted gene function listed. Some proteins in the family COG3984 (RamA-like) were found located next to carbon monoxide dehydrogenase (CODH) genes, suggesting they may play a role in the function of this complex instead. MAGs not listed did not have any methyltransferase genes encoded. Double slashes indicate the gene is truncated at the end of a scaffold. Each cluster of arrows depicted represents a separate scaffold. Locus tag(s) for genes on IMG are indicated in parentheses for each scaffold.

Supplementary Methods

Cell extractions and catalyzed reporter deposition fluorescence *in situ* hybridization (CARD-FISH)

Sediment samples from YNP sites LCB-003 and LCB-024 were collected in July 2019, fixed with paraformaldehyde at a final concentration of 2% for 8 h at 4°C, washed twice with 1x phosphate buffered saline (PBS) and stored in 1x PBS at 4 °C until cells were extracted. Extractions were performed by diluting aliquots of the sediment slurries 1:1 in PBS, adding methanol to a final concentration of 10%, Tween-20 to a final concentration of 0.1%, and vortexing the solution horizontally (Vortex-Genie2, Scientific Industries, Inc., Bohemia, NY) for five minutes to detach cells from particles. After vortexing, an equal volume of 80% (w/v) Nycodenz was layered under the sample and centrifuged at 16,000 g for 30 min at 4°C. Following centrifugation, the supernatant and interphase layers were transferred to a new tube, diluted 1:1 in PBS, and centrifuged at 16,000 g for 5 min to pellet the cells. The supernatant was removed, and the cells were resuspended in 1x PBS and stored at 4°C. Aliquots of the cell suspension were immobilized onto glass slides and CARD-FISH was performed as described in (1) with the following modifications. Cell permeabilization was attempted with either proteinase K (15 µg/mL) for 10 minutes or with 0.1 M HCl for 1 minute at room temperature. Endogenous peroxidases were inactivated by incubating in 0.01 M HCl for 15 minutes. A Culexarchaeaceae-specific probe, Culex824 (5'-TCCACCTAACACCTAGCC-3'), targeted at the 16S rRNA of Culexarchaeaceae found in terrestrial hot springs, was designed using the probe design tool within the Arb software and the Silva 132 reference database (2, 3). Hybridization of probe Culex824 was attempted at formamide concentrations 0, 10, 20, and 35 %. Positive and negative control hybridization reactions were performed with the general archaeal probe Arc915 (5'-GTGCTCCCCCGCCAATTCCT-3') and NON338 (5'-ACTCCTACGGGAGGCAGC-3'), respectively (4). All probes were labeled with horseradish peroxidase (HRP) and were purchased from Biomers (Ulm, Germany). Tyramide signal amplification was performed with Alexa Fluor 594 (Thermo Fisher). Samples were stained with DAPI, embedded in citifluor, and visualized under an epifluorescence microscope (Leica DM4B).

Supplementary results and discussion

Reclassification of JZ-bin-30

Based on our analyses, we propose to reclassify bin JZ-bin-30, originally given the provisional taxonomic assignment *Candidatus* Methanomedium jinzeense (5), as *Candidatus* Culexarchaeum jinzeense sp. nov. (etymology below). We base this re-assignment on the observation in 16S rRNA gene and phylogenomic analyses that JZ-bin-30 does not fall within the candidate class Methanomethylia, but rather within the new candidate class Culexarchaeia. Additionally, in contrast to what the name Methanomedium implies,

all currently available Culexarchaeia MAGs, including JZ-bin-30, lack the key enzyme for methanogenesis (methyl-coenzyme M reductase; Mcr) and lack methanogenesis marker genes that have been identified in both *bona fide* Euryarchaeotal methanogens and newly proposed MCR-encoding archaea outside the Euryarchaeota (6).

References

1. Hatzenpichler R, Lebedeva EV, Spieck E, Stoecker K, Richter A, Daims H, Wagner M. 2008. A moderately thermophilic ammonia-oxidizing crenarchaeote from a hot spring. *Proceedings of the National Academy of Sciences* 105:2134-2139.
2. Quast C, Pruesse E, Yilmaz P, Gerken J, Schweer T, Yarza P, Peplies J, Glöckner FO. 2012. The SILVA ribosomal RNA gene database project: improved data processing and web-based tools. *Nucleic acids research* 41:D590-D596.
3. Ludwig W, Strunk O, Westram R, Richter L, Meier H, Yadhukumar, Buchner A, Lai T, Steppi S, Jobb G. 2004. ARB: a software environment for sequence data. *Nucleic acids research* 32:1363-1371.
4. Ravensschlag K, Sahn K, Amann R. 2001. Quantitative molecular analysis of the microbial community in marine Arctic sediments (Svalbard). *Applied and Environmental Microbiology* 67:387-395.
5. Berghuis BA, Yu FB, Schulz F, Blainey PC, Woyke T, Quake SR. 2019. Hydrogenotrophic methanogenesis in archaeal phylum Verstraetearchaeota reveals the shared ancestry of all methanogens. *Proceedings of the National Academy of Sciences* 116:5037-5044.
6. Borrel G, Adam PS, McKay LJ, Chen L-X, Sierra-García IN, Sieber CM, Letourneur Q, Ghozlane A, Andersen GL, Li W-J. 2019. Wide diversity of methane and short-chain alkane metabolisms in uncultured archaea. *Nature microbiology* 4:603-613.